AD_____

Award Number: W81XWH-04-1-0407

TITLE: Examining the Role of Msh2 and Mre11 in Telomere Rescue

PRINCIPAL INVESTIGATOR: Damon Meyer, B.A.

CONTRACTING ORGANIZATION: Beckman Research Institute
Duarte CA 91010-3000

REPORT DATE: April 2007

TYPE OF REPORT: Annual Summary

PREPARED FOR: U.S. Army Medical Research and Materiel Command
Fort Detrick, Maryland 21702-5012

REPORT DOCUMENTATION PAGE

Form Approved
OMB No. 0704-0188

1. REPORT DATE *(DD-MM-YYYY)*	**2. REPORT TYPE**	**3. DATES COVERED** *(From - To)*
01-04-2007	Annual Summary	15 Mar 04 – 14 Mar 07

4. TITLE AND SUBTITLE
Examining the Role of Msh2 and Mre11 in Telomere Rescue

5a. CONTRACT NUMBER

5b. GRANT NUMBER
W81XWH-04-1-0407

5c. PROGRAM ELEMENT NUMBER

6. AUTHOR(S)
Damon Meyer, B.A.

E-Mail: dmeyer@coh.org

5d. PROJECT NUMBER

5e. TASK NUMBER

5f. WORK UNIT NUMBER

7. PERFORMING ORGANIZATION NAME(S) AND ADDRESS(ES)

Beckman Research Institute
Duarte CA 91010-3000

8. PERFORMING ORGANIZATION REPORT NUMBER

9. SPONSORING / MONITORING AGENCY NAME(S) AND ADDRESS(ES)
U.S. Army Medical Research and Materiel Command
Fort Detrick, Maryland 21702-5012

10. SPONSOR/MONITOR'S ACRONYM(S)

11. SPONSOR/MONITOR'S REPORT NUMBER(S)

12. DISTRIBUTION / AVAILABILITY STATEMENT
Approved for Public Release; Distribution Unlimited

13. SUPPLEMENTARY NOTES

14. ABSTRACT: Tumorigenesis is characterized by genome instability that results in genetic changes that promote a cancerous state1. Instability at telomeres can result in "uncapping" of the ends of linear chromosomes, making them vulnerable to recombination, mutation and gross-chromosomal rearrangement (GCR)2,3,4. Continuously dividing human somatic cells and S. cerevisiae cells lacking functional telomerase, a ribonucleoprotein complex required for telomere replication, experience progressive telomere degradation that culminates in replicative senescence5,6. Our research has shown that during replicative senescence genes located proximal to telomeres experience increases in mutationand GCR that are dependent on the error-prone polymerase genes REV1 and REV7. Interestingly, viability is increased and replicative senescence is delayed in telomerase deficient diploid cells. This may be because the presence of a homologous chromosome provides the opportunity to rescue defective chromosomes by inter-homolog exchange (IHE), or to tolerate their loss. In support of this idea both IHE and chromosome loss (CL) increase during replicative senescence. Senescence-associated IHE is dependent on the central homologous recombination gene, RAD52, but is independent from the error-prone polymerase genes REV1 and REV7. Finally, we have identified a new role for telomerase in facilitating the formation of translocations after double-strand breaks are made on two different chromosomes.

15. SUBJECT TERMS
Genetics,Molecular Biology,DNA Repair,Homologous Recombination,Genome Instability,Telomere Rescue, Msh2, Mre11/Rad50/Xrs2,Replication Failure,Error-prone polymerases,GCR,

16. SECURITY CLASSIFICATION OF:			**17. LIMITATION OF ABSTRACT**	**18. NUMBER OF PAGES**	**19a. NAME OF RESPONSIBLE PERSON**
a. REPORT	**b. ABSTRACT**	**c. THIS PAGE**			USAMRMC
U	U	U	UU	46	**19b. TELEPHONE NUMBER** *(include area code)*

14. ABSTRACT: Tumorigenesis is characterized by genome instability that results in genetic changes that promote a cancerous state1. Instability at telomeres can result in "uncapping" of the ends of linear chromosomes, making them vulnerable to recombination, mutation and gross-chromosomal rearrangement (GCR)2,3,4. Continuously dividing human somatic cells and S. cerevisiae cells lacking functional telomerase, a ribonucleoprotein complex required for telomere replication, experience progressive telomere degradation that culminates in replicative senescence5,6. Our research has shown that during replicative senescence genes located proximal to telomeres experience increases in mutationand GCR that are dependent on the error-prone polymerase genes REV1 and REV7. Interestingly, viability is increased and replicative senescence is delayed in telomerase deficient diploid cells. This may be because the presence of a homologous chromosome provides the opportunity to rescue defective chromosomes by inter-homolog exchange (IHE), or to tolerate their loss. In support of this idea both IHE and chromosome loss (CL) increase during replicative senescence. Senescence-associated IHE is dependent on the central homologous recombination gene, RAD52, but is independent from the error-prone polymerase genes REV1 and REV7. Finally, we have identified a new role for telomerase in facilitating the formation of translocations after double-strand breaks are made on two different chromosomes.

Table of Contents

Cover……1

SF 298……2

Introduction……5

Body……5

Key Research Accomplishments……7

Reportable Outcomes……7

Conclusions……8

References……8

Bibliography……8

Appendices……10

Introduction: Tumorigenesis is characterized by genome instability that results in genetic changes that promote a cancerous state[1]. Instability at telomeres can result in "uncapping" of the ends of linear chromosomes, making them vulnerable to recombination, mutation and gross-chromosomal rearrangement (GCR)[2,3,4]. Continuously dividing human somatic cells and *S. cerevisiae* cells lacking functional telomerase, a ribonucleoprotein complex required for telomere replication, experience progressive telomere degradation that culminates in replicative senescence[5,6]. Our research has shown that during replicative senescence genes located proximal to telomeres experience increases in mutations and GCR that are dependent on the error-prone polymerase genes *REV1* and *REV7*. Interestingly, viability is increased and replicative senescence is delayed in telomerase deficient diploid cells. This may be because the presence of a homologous chromosome provides the opportunity to rescue defective chromosomes by inter-homolog exchange (IHE), or to tolerate their loss. In support of this idea both IHE and chromosome loss (CL) increase during replicative senescence. Senescence-associated IHE is dependent on the central homologous recombination gene, *RAD52*, but is independent from the error-prone polymerase genes *REV1* and *REV7.* Finally, we have identified a new role for telomerase in facilitating the formation of translocations after double-strand breaks are made on two different chromosomes.

Body:

I. *Creation of est2 mutant strains and examining role of msh2 in ALT*

I have created two *est2* mutant strains by disrupting the *EST2* coding sequence with one of two selectable prototrophic markers, *URA3* or *LEU2*, resulting in *est2::URA3* and *est2::ura3::LEU2.* These allow for the use of two different selectable markers when creating mutant strains with *MSH2* and/or *MRE11*. In addition, the *est2 msh2* double mutant and the *est2 msh2 mre11, est2 msh2 rad51* and *est2 mre11 rad51* triple mutants have been created.

I have done serial liquid growth and serial streaking experiments on YPD plates with wild-type, *est2* and *est2 msh2* strains. In addition, cell viability was determined each day in liquid culture (Fig. 1 and 2, Appendices). It appears from the data that *est2 msh2* double mutants fail to lose viability during senescence to the same extent observed in the *est2* mutants. This is most evident when examining cell viability in Fig. 2, which requires single cells to form a colony on YPD plates unlike the serial liquid growth assay that counts just cell bodies. Plating efficiency in *est2 msh2* double mutants drops to around 25-35% during senescence and remains below 50% until 100 generations, unlike *est2* mutants that show a plating efficiency of approximately 2% during senescence and quickly improves to wild type levels by 60-70 generations. Therefore, the *est2* single and *est2 msh2* double mutants senesce and recover with distinctly different kinetics.

I examined survivors of *est2* and *est2 msh2* strains to determine the ratio of Type I/ Type II survivors and if loss of *MSH2* changes that ratio. The results are derived from survivors in liquid culture and from plates. In *est2* survivors the relative ratio of Type I/ Type II survivors is 23/50 = .46. However, *est2* msh2 survivors have a relative ratio of Type I/ Type II survivors of 33/1 = 33 a significant shift from that observed in *est2* survivors. These data suggest that Msh2 is either involved in restricting Type I survivors or promoting Type II survivors. This difference can only be addressed upon final examination of *est2 msh2 rad51* and *est2 msh2 mre11* triple mutants.

II. *Measuring Genome Instability by Inter-homolog Recombination, Chromosome Loss, Mutations & Gross Chromosomal Rearrangements at a Telomere-linked Locus.*

As *est2* mutants progress toward senescence it is thought that telomeres progressively shorten leading to a loss of "capping" and thus DNA end protection. The loss of DNA end protection leads to unfavorable genomic rearrangements and ultimately, replicative senescence. This genomic instability also occurs in human somatic cells that have continued to divide beyond the normal control of cell growth. These cells are precursors in cancer development. Although most die, a few may potentially acquire genetic changes that allow them to progress toward a cancerous state, which includes ALT-dependent cancer. Therefore, it is of interest to study senescence-associated genomic instability, by examining mutations, IHR, CL, and gross chromosomal rearrangements (GCR).

One way to think about the progression toward cancer is as a series of events that first introduce mutations into genes that control cell growth, and, second, result in loss of the unaltered copies of those genes (loss of heterozygosity-LOH) such that growth control is disrupted. Since cancer is a disease of the aged and replicative

senescence is a process that has been proven to destabilize the genome, we examined the link between replicative senescence and events that are associated with the development of cancer. First, we examined how replicative senescence influences mutations and GCR, which are events that could disrupt the function of genes in response to telomere failure. The GCR/mutation assay, (see attached manuscript, Meyer Genetics), uses two markers, *CAN1* and *hxt13::URA3*, located 32kb and 21kb away from the telomere on the left end of chromosome V respectively. We found that there was a 16-fold increase in the mutation rate and a 383-fold increase in the rate of GCR at the *CAN1* locus concurrent with senescence. Importantly, there was no increase in the mutation rate at the *CYH2* locus that lies 320 kb from the telomere on the right arm of chromosome VII, suggesting that the mutagenic effects of telomere failure are a function of distance from the telomere. Furthermore, we found that *REV1* and *REV7* are necessary for increased GCR and mutation during senescence, and that *RAD30* suppresses it. This suggests that DNA replication may be disrupted near telomeres during replicative senescence. This work changes the way we view the relationship between telomere dynamics and genome stability, and how these dynamics may contribute to cancer.

LOH, by recombination between homologs, or chromosome loss could serve to establish the homozygosity of mutations generated during senescence, thereby contributing to the progression toward cancer. We examined the link between replicative senescence and LOH using the IHR/CL assay (Fig. 3, Appendices). The IHR/CL assay makes use of two selectable markers on opposite ends of the centromere on chromosome V. Loss of both selectable markers is counted as a CL event while loss of one marker is counted as an IHR event. The most significant observations were that the *est2* diploids displayed increases in IHR and CL of 16- and 7-fold, respectively, during senescence but not before or after. This suggests that replicative senescence results in the accumulation of lesions, such as a double-strand break (DSB) that can stimulate both types of events. Further, while the increased IHR and CL conferred by the *est2* mutation appeared to be more or less independent of the error prone polymerases, the IHR was highly dependent on *RAD52*, while CL appeared to be stimulated by its loss. This is consistent with *RAD52* being required to generate the IHR events using the lesions that accumulate in *est2* mutant cells that will otherwise result in chromosome loss.

The accumulation of DSBs that increases IHR and CL during replicative senescence in *est2* diploid cells might be expected to negatively affect the growth of senescent *est2* haploid cells because they lack the homolog with which to either fix the broken chromosome by recombination, or, complement its loss. Therefore, *est2* mutant diploids might be expected to survive replicative senescence better than *est2* haploids. We tested this by comparing the viability of *est2* haploids and diploids (Figure 4, Appendices). The diploids both senesce later (60 vs. 40 generations) and display greater viability during senescence (15% vs. 1%) than the haploids, consistent with the homolog affecting both the rate of replicative senescence and the severity of its effects. Viability of *rad30, rev7, est2 rad30* and *est2 rev7* diploids were determined and looked like either wild-type (*rad30* and *rev7*) or *est2* diploids (*est2 rad30* and *est2 rev7*) (data not shown).
Interestingly, the presence of a homolog does not improve the growth of *est2 rad52* double mutant diploids, suggesting that the capacity to perform homologous recombination between the homologs contributes significantly to the improved survivorship of *est2* diploids.

Homologous recombination had previously been shown to be under the control of the mating type locus in yeast[7], suggesting that improved survivorship in the *est2* diploid may not be due to the presence of a homolog, but instead heterozygosity at the mating type locus. To test this we constructed diploid strains that were homozygous for mating type, either a/a or α/α, and haploids that were heterozygous for mating type (a/α). The results (Figure 5 & 6, Appendices) showed that in fact the presence of the homolog is the primary determining factor for the delay and improved viability in senescent *est2* mutants. In addition, Figure 5 shows that a mating type of a/α in a haploid plays some role in improving viability during senescence, but not delaying senescence, which has been observed previously[7].

III. Measuring the Frequency of Translocation

We found that loss of *EST2* stimulates GCR, which can include translocations[8]. In order to determine if the *est2* mutation has an effect on translocation formation by homologous recombination we measured the frequency of translocation resulting from two HO-endonuclease generated double-strand breaks (Figure 7, Appendices). The translocation assay makes use of HO cut sites at the *his3Δ3'* substrate on chromosome XV, and the *his3Δ5'* substrate on chromosome III, and selects for the generation of an intact *HIS3* sequence by a translocation event. Our results (Figure 8, Appendices) show that both *est2* and *tlc1* mutations confer a significant 20-fold reduction in translocations independent of replicative senescence. Since previous work in the lab has shown evidence that translocations are

due to single-strand annealing we also tested if *EST2* played a role in direct repeat recombination, which is dependent on single-strand annealing. The direct-repeat assay measures the generation of an intact *HIS3* sequence by recombination between two truncated *his3* genes that share 103 bp or 415 bp of homology, and are separated by a selectable *URA3* gene. Our results (Figure 9, Appendices) showed that direct repeat recombination is slightly but significantly decreased in *est2* mutants. All assays were conducted in pre-senescent cells. These results suggest a novel role for *EST2* in double-strand break repair.

Key Research Accomplishments:

- Generated an *est2::ura3::LEU2* that uses a new marker to follow *est2* mutants.
- Recapitulated results by Rizki & Lundblad (2001) showing *est2 msh2* cells grow better than *est2* during the time of senescence in liquid culture .
- Showed cell viability in *est2 msh2* double mutants is low but stable at around 25-35%, has a delayed recovery around 100-110 generations.
- Cell viability in *est2* mutants follow a similar pattern of cell growth, senescence and recovery observed in serial liquid growth.
- The relative ratio of Type II/I survivors in *est2* mutants is 23/50 = 0.46.
- The relative ratio of Type II/I survivors in *est2 msh2* double mutants is 33/1 = 33.
- Completed all cloning steps needed for the creation of the telomere construct.
- Created an *est2*/*est2* and wild type chromosome loss strain.
- Showed a 17-fold increase in the mutation rate of a telomere proximal gene in est2 mutants during the time of senescence. Furthermore, the mutation rate of a telomere proximal gene decreased to wild-type levels during survivor formation.
- Showed a 383-fold increase in the GCR rate in est2 mutants of telomere proximal sequences within 32kb of the telomere. This increased occurred during senescence and progressively decreased during the advent of survivor formation to wild type levels by ~125 generations.
- *est2 rev1* and *est2 rev7* double mutants show no increase in mutation or GCR during the time of senescence. This suggests a role of both Rev1 and Rev7 in generating GCR and mutation.
- *est2 rad30* mutants have a 37-fold increase in the GCR rate during the first testable time point relative to wild type. This enhanced increase is maintained during senescence to 2300-fold above wild type.
- Exo1 has no affect in the increases in GCR or mutation.
- Mutation increases during senescence of *est2* mutants does not occur in loci that are not telomere proximal.
- Mutation spectra are the same in wild type and *est2* mutants.
- IHR and CL in *est2, est2 rev7,* and *est2 rad30* are significantly above wild-type during replicative senescence.
- CL in *rad52* is significantly increased above wild-type.
- IHR but not CL in *est2 rad52* is significantly decreased from wild-type.
- Diploid *est2* serial cultures show a delay and improved viability from a haploid *est2* serial cultures that is due to the presence of the homolog.
- *est2* showed a decrease in translocation and direct-repeat indicating a role in single-strand annealing.

Reportable Outcomes: 1 manuscript, in press *Genetics* (see attached).

Conclusions:

Understanding the impact of telomere instability and replicative senescence may be critical to understanding the relationship between aging and cancer. Our results show a significant increase in mutation, LOH and genome rearrangement during senescence in *est2* mutant cells. It seems probable that the population of cells that emerge from senescence are more likely to possess genetic changes that impact their growth control. Given that they are already capable of growing without the restrictions imposed by dependence on telomerase, it seems likely that cells that emerge from senescence will be more tumorigenic. Additonally, these results have implications with regard to the evolution of gene location along linear chromosomes, as genes located close to telomeres could be

differentially susceptible to mutation and LOH. Therefore, genomes may have evolved such that essential genes are located away from the telomere.

Our results with diploid yeast cells suggest that the presence of homologous chromosome could stabilize the genome and delay replicative senescence in human somatic cells. However, increased LOH during senescence in diploids suggests that deleterious recessive mutations arising during senescence are more likely to become homozygous, supporting the idea that the cells of elderly people are more likely to undergo the genome destabilization that fuels cancer.

"So What"

These results are helping to understand the progression of telomerase null somatic cells toward cancer. This will help to identify molecular targets for drugs that kill these unique ALT cancer cells that would be immune to telomerase inhibitors.

Reference:

1. Michor, F., Iwasa, Y., Vogelstein, B., Lengauer, C. & Nowak, M.A. Can chromosomal instability initiate tumorigenesis? *Semin. Cancer Biol.* **15,** 43-49 (2005).
2. Hackett, J.A. & Greider, C.W. End resection initiates genomic instability in the absence of telomerase. *Mol. Cell. Biol.* **23,** 8450-8461 (2003).
3. Hackett, J.A., Feldser, D.M. & Greider, C.W. Telomere dysfunction increases mutation rate and genomic instability. *Cell* **106,** 275-286 (2001).
4. DuBois, M.L., Haimberger, Z.W., McIntosh, M.W. & Gottschling, D.E. A quantitative assay for telomere protection in *Saccharomyces cerevisiae*. *Genetics* **161,** 995-1013 (2002).
5. Lendvay, T.S., Morris, D.K., Sah, J., Balasubramanian, B. & Lundblad, V. Senescence mutants of *Saccharomyces cerevisiae* with a defect in telomere replication identify three additional *EST* genes. *Genetics* **144,** 1399-1412 (1996).
6. Neumann, A.A. & Reddel, R.R. Telomere maintenance and cancer – look, no telomerase. *Nat Rev. Cancer* **2,** 879-884 (2002).
7. Lowell J.E., Roughton A.I., Lundblad V., Pillus L. Telomerase-independent proliferation is influenced by cell type in Saccharomyces cerevisiae. *Genetics* **164,** 909-921 (2003).
8. Myung, K., Chen, C. & Kolodner, R.D. Multiple pathways cooperate in the suppression of genome instability in *S. cerevisiae*. *Nature* **411,** 1073-1076 (2001).

Bibliography:

Poster presentation: **D. Meyer**, A. M. Bailis. Induction of mutagenesis and gross chromosomal rearrangements during telomere degradation. 4th Era of Hope meeting, Department of Defense (DOD) Breast Cancer Research Program (BCRP), June 8-11, Philadelphia, Pennsylvania. (2005)

Research presentation: **D. Meyer.** Control of GCR and Mutation by Error Prone Polymerases During Replicative Senescence in Telomerase Deficient Cells. City of Hope Research Staff Organization Advance, Lake Arrowhead, CA. (2006)

D. Meyer and A. M. Bailis. Telomere Dysfunction Drives Increased Mutation by Error-Prone Polymerase ζ in *Saccharomyces cerevisiae.* ***Genetics*** (In Press)

List Receiving Pay For Research Effort:

Damon H. Meyer, Graduate Student

Telomere Dysfunction Drives Increased Mutation by Error-Prone Polymerases Rev1 and ζ in *Saccharomyces cerevisiae.*

Damon H. Meyer*,□ & Adam M. Bailis*, 1

*,1 *Division of Molecular Biology,*

Beckman Research Institute of the City of Hope,

Duarte, CA. 91010-0269

□ *City of Hope Graduate School of Biological Sciences*

Genetics: Published Articles Ahead of Print, published on December 6, 2006 as 10.1534/genetics.106.068130

Running Head: Telomere Dysfunction Drives Mutation

Key Words: Telomere, Mutation, Error-prone polymerases, replication, GCR

1 **Corresponding Author:** Adam M. Bailis, Ph.D. Division of Molecular Biology, Beckman Institute of the City of Hope, 1450 E. Duarte Rd., Duarte, CA 91010-0269. Phone: (626) 359-8111 x64031, Fax: (626)930-5463, E-mail: abailis@bricoh.edu.

Using a model system, we have shown that replicative senescence is accompanied by a 16-fold increase in base substitution and frameshift mutations near a chromosome end. The increase was dependent on error-prone polymerases required for the mutagenic response to DNA lesions that block the replication fork.

LEAVE BLANK

S. cerevisiae cells lacking telomerase, a ribonucleoprotein complex required for telomere replication, experience progressive telomere degradation that culminates in replicative senescence (Lendvay *et al.* 1996). Deletions that encompass the *CAN1* locus located approximately 32 kb from the telomere on the left arm of chromosome V accumulated during senescence (Hackett and Greider 2003; Hackett *et al.* 2001), and have been attributed to replication fork stalling (Motegi *et al.* 2006). Since replication fork stalling also generates mutations (Quah *et al.* 1980), we investigated the effect of telomere dysfunction on the generation of mutations at the *CAN1* locus.

Mutation Rate Analysis:

We examined the behavior of mutants defective for *EST2,* which encodes the catalytic subunit of telomerase (Counter *et al.* 1997). We determined the mutation rate at the *CAN1* locus using an assay that selects against deletions in serial cultures of wild type and *est2* mutant cells. We observed no significant change from the wild type rate of *CAN1* mutation in *est2* cultures before senescence ($p = 0.07$), a 16-fold increase during senescence ($p < 0.0001$) and the restoration of wild type levels upon recovery ($p = 0.09$) (Fig. 1a). No senescence-dependent changes in the mutation rate at the *CYH2* locus, located 310 kb from its telomere on the left arm of chromosome VII, were observed in *est2* mutant cultures before ($p = 0.68$), during ($p = 1.0$), or after replicative senescence ($p= 1.0$) (Fig. 2), suggesting that the mutagenic effect is restricted to telomere proximal sequences. The *can1* mutation spectrum observed for senescent *est2* mutant cells was similar to that of wild type (Table 2), suggesting that the mechanism of senescence-dependent

mutagenesis in *est2* cells may be similar to the mechanism of spontaneous mutagenesis in wild type cells. Since 50-70% of spontaneous mutagenesis has been attributed to the action of error-prone polymerases (Quah *et al.* 1980), we investigated whether they were involved in the mechanism underlying senescence-dependent mutagenesis. We examined the effects of mutations in the *RAD30, REV7* and *REV1* genes, which are required for error-prone polymerase function in yeast (Goodman 2002; Johnson *et al.* 2000; Haracska *et al.* 2000; Prakash *et al.* 2005). Mutation rates in *est2 rad30* cultures before ($p = 0.32$), during ($p = 0.34$) and after senescence ($p = 0.15$) were not significantly different than in *est2* cultures (Fig. 1a, 1b), suggesting that Pol｜ does not contribute to senescence dependent mutagenesis. In contrast the *rev1* and *rev7* mutations completely suppressed senescence-dependent mutagenesis, as the *CAN1* mutation rates were not significantly different from *rev1* and *rev7* mutants before ($p = 0.46$ *rev1*, $p = 0.53$ *rev7*), during ($p = 0.84$ *rev1*, $p = 0.09$ *rev7*) or after senescence ($p =$

1.0 *rev1*, p = 0.2 *rev7*) (Fig. 1a, 1b). Southern blot analysis of representative canavanine resistant mutants collected from senescent cells revealed that all had unrearranged *can1*

λοχι, χονσιστεντ ωιτη βασε συβστιτυτιον ανδ φραμεσηιφτ μυτατιονσ (ΔΜ ανδ ΑΒ, υνπ υβλισηεδ δατα). Τηεσε δατα συγγεστ τηατ Ρεϖ1 ανδ ΔΝΑ πολψμερασε ζ are required for senescence-dependent mutagenesis, perhaps through mutagenic bypass of DNA replication lesions generated during replicative senescence. The minimal effects of the *rad30*, *rev1* and *rev7* mutations on the growth, senescence and recovery of *est2 rad30*, *est2 rev1*, and *est2 rev7* cells (Fig.3a, 3b), suggest that the mutation of telomere-proximal sequences does not contribute to the initiation of, or recovery from senescence.

Exo1 has been suggested to be necessary for destabilizing the *CAN1* locus during senescence by promoting exonucleolytic degradation from the telomere (Hackett and Greider 2003). We observed no significant change in the rates of *CAN1* mutation in *est2 exo1* cultures before (p = 0.89) or after senescence (p = 1.0) from that observed in *exo1*

cultures, but did see a significant 10-fold increase during senescence ($p < 0.0001$)(Fig 1a,1b). These data suggest that Exo1-dependent nucleolytic degradation is not required toobserve senescence-dependent increases in *CAN1* mutation rate.

GCR Analysis:

In addition to mutagenesis, we also examined the rate of gross chromosomal rearrangement (GCR) in *est2* mutants grown serially over time. GCR is defined as an event that leads to the simultaneous loss of *CAN1* and a *URA3* marker inserted at the *HXT13* locus that lies between *CAN1* and the telomere on the left end of chromosome V (Chen and Kolodner 1999). The GCR rate was only two-fold over wild type before senescence, 383-fold over wild type during senescence, and decreased to wild type levelsupon recovery from senescence (Table 3), all consistent with previously published reports(Myung *et al.* 2001; Pennaneach and Kolodner 2004; Hackett *et al.* 2001). Consistent with *CAN1* mutagenesis *REV1* and *REV7* were found to be important in determining the GCR rate during replicative senescence. GCR rates in *est2 rev1* and *est2 rev7* mutants were only 2-4 fold higher during senescence than in *rev1* and *rev7* mutants (Table 3) that did not undergo senescence (Fig. 3a). These results are consistentwith Pol ζ and Rev1 being required for senescence-dependent GCR. Strikingly, Rad30was found to be required to suppress GCR as the rate in *est2 rad30* cells was 37-foldoverwild type before senescence, 2,673 fold over wild type during senescence and at wild

type levels upon recovery (Table 3). Interestingly, this increase is nearly completely dependent on Rev7 as the GCR rate in senescent *est2 rad30 rev7* cells was less than 2-fold greater than in the *est2 rev7* mutant (Table 3). Therefore, like senescence-dependentmutagenesis at the *CAN1* locus, senescence-dependent GCR requires Rev1 and Pol ζ.Our data suggest that Rev1- and Pol ζ-dependent mutations and GCR at telomereproximal loci are an important consequence of telomere dysfunction. The involvement ofPol η, Polζ and Rev1 suggests that the post-replication repair machinery (Minesinger andJinks-Robertson 2005) may be responding to the failure of bidirectional DNA replicationin the region (Lehmann 2005; Plosky and Woodgate 2004). Strathern and colleagueshave reported the involvement of Pol ζ in generating mutations associated with therecombinational repair of an enzyme-catalyzed double-strand break (Rattray et al. 2002),suggesting that a similar process may be involved in generating mutations at sequenceslying near the uncapped telomeres of senescent cells (Dubois *et al.* 2002). However,such a mechanism is unlikely to involve extensive exonucleolytic degradation from thetelomere as loss of Exo1, a factor involved in the degradation of uncapped telomeres(Hackett and Greider 2003), does not reduce senescence-dependent mutation (Fig. 1B) orGCR (Table 3). Further, this mechanism would likely require homologousrecombination between sister-chromatids, as the *CAN1* gene is a unique sequence in thegenome. Perhaps, similar forces underlie some of the increased genome instability andcancer in somatic cells of elderly people (Lengauer *et al.* 1998; Johnson *et al.* 1999).

ACKNOWLEDGEMENTS

We thank D. Gottschling, J. McDonald, R. Woodgate and V. Lundblad for supplying strains and plasmids. We also thank J. Termini, T. O'Connor and R-J Lin, and the members of the Bailis lab for productive discussions. Our thanks also go to several anonymous reviewers for their valuable comments. This work was supported by funds from the Beckman Research Institute of the City of Hope, the National Institutes of Health (GM057484 to A. B.) and the Dept. of Defense Breast Cancer Research Program (W81XWH0410407 to D. M.).

LITERATURE CITED

Chen C. & Kolodner, R.D., 1999 Gross chromosomal rearrangements in *Saccharomyces*
cerevisiae replication and recombination defective mutants Nature **23**: 81-85.

Counter, C. M., M. Meyerson, E.N. Eaton and R.A. Weinberg, 1997 The catalytic subunit
of yeast telomerase. Proc Natl Acad Sci USA **94:** 9202-9207.
DuBois, M.L., Haimberger, Z.W., McIntosh, M.W. and D. E. Gottschling, 2002 A quantitative assay for telomere protection in *Saccharomyces cerevisiae.* Genetics **161:**995-1013.
Goodman, M. F., 2002 Error-prone repair DNA polymerases in prokaryotes and eukaryotes. Annu. Rev. Biochem. **71:** 17-50.
Hackett, J. A., and C. W. Greider, 2003 End resection initiates genomic instability in the absence of telomerase. Mol. Cell. Biol. **23:** 8450-8461.
Hackett, J. A., D. M. Feldser and C. W. Greider, 2001 Telomere dysfunction increases mutation rate and genomic instability. Cell **106:** 275-28.

Haracska, L., S.- L.Yu, R. E. Johnson, L. Prakash and S. Prakash, 2000 Efficient and accurate replication in the presence of 7,8-dihydro-8-oxoguanine by DNA polymerase eta. Nat. Genet. **25:** 458–461.

Johnson, R. E., C. M. Kondratick, S. Prakash and L. Prakash, 1999 hRAD30 mutations in
the variant form of xeroderma pigmentosum. Science **285:** 263-265.
Johnson, R. E., M. T. Washington, S. Prakash and L. Prakash, 2000 Fidelity of human DNA polymerase eta. J. Biol. Chem. **275:** 7447–7450.
Lea, D. E., and C. A. Coulson, 1949 The distribution of the numbers of mutants in bacterial populations. J. Genet. **49:** 264-285.
Lehmann, A. R., 2005 Replication of damaged DNA by translesion synthesis in human cells. FEBS Lett. **579:** 873-876.
Lendvay, T. S., D. K. Morris, J. Sah, B. Balasubramanian and V. Lundblad, 1996 Senescence in mutants of *Saccharomyces cerevisiae* with a defect in telomere replication identify three additional EST genes. Genetics **144:** 1399-1412.
Lengauer, C., K. W. Kinzler and B. Vogelstein, 1998 Genetic instabilities in human cancers. Nature **396:** 643-649.
Luria, S. E., and M. Delbruck, 1943. Mutations of bacteria from virus sensitivity to virus resistance. Genetics **28:** 491-511.
Minesinger, B. K., and S. Jinks-Robertson, 2005 Roles of RAD6 epistasis group members in spontaneous pol zeta-dependent translesion synthesis in *Saccharomyces cerevisiae*. Genetics. **169:** 1939-1955.
Motegi, A., K. Kuntz, A. Majeed, S. Smith and K. Myung, 2006 Regulation of gross

chromosomal rearrangements by ubiquitin and SUMO ligases in *Saccharomyces cerevisiae.* Mol. Cell. Biol. **26:** 1424-1433.
Myung, K., C. Chen and R. D. Kolodner, 2001 Multiple pathways cooperate in the suppression of genome instability in *Saccharomyces cerevisiae.* Nature **411:** 1073-1076.
Pennaneach, V., and R. D. Kolodner, 2004 Recombination and the Tel1 and Mec1 checkpoints differentially effect genome rearrangements driven by telomere dysfunction in yeast. Nat. Gen. **36:** 612-61.
Plosky, B. S., and R. Woodgate, 2004 Switching from high-fidelity replicases to lowfidelity
lesion-bypass polymerases. Curr. Opin, Genet. Dev. **14:** 113-119.
Prakash, S., R. E. Johnson and L. Prakash, 2005 Eukaryotic translesion synthesis DNA polymerases: specificity of structure and function. Annu. Rev. Biochem. **74:** 317-353.
Quah, S.- K., R. C. Von Borstel and P. J. Hastings, 1980 The origin of spontaneous mutation in *Saccharomyces cerevisiae*. Genetics **96:** 819-839.
Rattray, A. J., B. K. Shafer, C. B. McGill and J. N. Strathern, 2002 The Roles of *REV3* and *RAD57* in Double-Strand-Break-Repair-Induced Mutagenesis of *Saccharomyces cerevisiae*. Genetics **162:** 1063-1077.

Table 1: *S. cerevisiae* Strains Used in this Study

Strain	Genotype
ABX1269	*MATa/α ade2-1/ade2-1 CAN1/can1-100 HIS3/his3-11, 15 leu2-3, 112/ leu2-3, 112 trp1-1/trp1-1 ura3::TRP1/ura3::TRP1 HXT13/hxt13::URA3 EST2/est2::LEU2 EXO1/exo1::hisG RAD5/RAD5*
ABX1429	*MATa/α ade2-101/ade2-1 can1-100/can1-100 his3-Δ200/his3-11, 15 leu2-Δ1/leu2-3, 112 trp1-1/trp1-1 ura3-52/ura3-1 adh4::URA3-TEL/ ADH4 CYH2/CYH2 EST2/est2::LEU2 RAD5/RAD5*
ABX1727	*MATa/α ade2-1/ade2-1 CAN1/CAN1 HIS3/his3-11, 15 leu2-3, 112/ leu2-3, 112 trp1-1/trp1-1 ura3::TRP1/ura3::TRP1 hxt13::URA3/ hxt13::URA3 EST2/est2::LEU2 REV1/rev1::HIS3 RAD5/RAD5*
ABX1729	*MATa/α ade2-1/ade2-1 CAN1/CAN1 his3-11, 15/his3-11, 15 leu2-3, 112/ leu2-3, 112 trp1-1/trp1-1 ura3::TRP1/ura3::TRP1 hxt13::URA3/ hxt13::URA3 EST2/est2::LEU2 RAD30/rad30::HIS3 REV7/rev7::hisG RAD5/RAD5*

Table 2: *CAN1* Mutation Spectra in Wild type and Mutant Cells [a]

Mutation Type				
Genotype	Base Substitution	Frame-shift	Insertion/Deletion	Complex
Wild type	50%	43.7%	0%	6.25%
est2	50%	50%	0%	0%

[a] Genomic DNA was extracted from 32 independent *can1* mutant colonies derived from wild type cells and 22 independent *can1* mutant colonies derived from senescent *est2* mutant cells and used to program PCR reactions to amplify the 2 kb *CAN1* sequence using primers 101 (5'CTC GAG TTT ACG TAT ATA TCT GGA ACA G) and 102 (5'CTC GAG GGG TGA GAA TGC GAA ATG GCG). PCR products were purified and subjected to sequencing using primers 201 (5'TAT TGG TAT GAT TGC CCT TG), 202 (5'GAG TTC TGG GTC GCT TCC ATC), 203 (5'CAA TCT ACT TCC TAC GTT TC), 204 (5'GAA TAT GCC AAA GAA CCC) and 205 (5'GAG GGT GAG AAT GCG AAA

T).

Table 3: Control of Senescence-Dependent Gross Chromosomal Rearrangement

Genotype	GCR Rate[a] 25generations[b]	50 generations[c]	150 generations[d]
Wild type	1.73 x 10^{-9}	1.07 x 10^{-9}	1.98 x 10^{-9}
est2	4.36 x 10^{-9} (2.5)[e]	4.1 x 10^{-7} (383)	4.93 x 10^{-9} (2.5)
exo1	1.74 x 10^{-8} (10)	4.73 x 10^{-9} (4.5)	7.5 x 10^{-9} (4)
rad30	3.4 x 10^{-9} (2)	2.56 x 10^{-9} (2)	2.11 x 10^{-9} (1)
rev1	1.44 x10^{-9} (8)	1.45x10^{-9} (13)	7.56 x 10^{-9} (4)
rev7	1.01 x 10^{-9} (6)	9.65 x 10^{-9} (9)	7.56 x 10^{-9} (4)

est2 exo1 1.2 x 10^{-8} (7) 3.19 x 10^{-7} (298) 1.31 x 10^{-8} (6.5)

est2 rad30 6.39 x 10^{-9} (37) 2.86 x 10^{-6} (2,673) 4.55 x 10^{-9} (2)

est2 rev1 8.84 x 10^{-9} (5) 3.1 x 10^{-8} (29) 1.53 x 10^{-8} (8)

est2 rev7 1.24 x 10^{-8} (7) 4.0 x 10^{-8} (37) 1.6 x 10^{-8} (8)

rad30 rev7 4.1 x 10^{-9} (2) 3.9 x 10^{-9} (3.5) 2.4 x 10^{-9} (1)

est2 rad30 rev7 4.7 x 10^{-8} (27) 6.95 x 10^{-8} (65) 5.79 x 10^{-9} (3)

[a] Fresh spore colonies of the appropriate genotype were taken in their entirety from the dissection plate and dispersed in water. Aliquots were removed to determine viability following dilution, plating on to YPD medium and incubation at 30° for three days. The remainder was plated on to synthetic medium containing canavanine and allowed to form colonies at 30°C, at which point colonies were counted and replica plated on to synthetic medium lacking uracil. GCRs were defined as the canavanine resistant cells that had lost the ability to grow without uracil. The deletion rate was determined by fluctuation analysis (Luria and Delbruck 1943). Five subsequent serial calculations of the GCR rate were performed using single colonies arising on the YPD viability plates.

[b] Deletion rate before replicative senescence, ~25 generations.

[c] Deletion rate during replicative senescence, ~50 generations.

[d] Deletion rate after recovery from replicative senescence, ~150generations.

[e] Fold differences from wild type level at a comparable number of generations in parentheses.

FIGURE LEGENDS

Figure 1. *REV1* and *REV7*, but not *RAD30* are required to observe increases in *CAN1* mutation rate during replicative senescence in *est2* mutant cells. **a**. *CAN1* mutation rate of ▲ wild type, ☐ *est2*⊗, ☐ *rev1*⊗, ☐ *rev7*⊗, ☐*rad30*⊗ and ◆ *exo1*⊗ mutant cells at the
indicated time points. **b**. *CAN1* mutation rate of ☐ *est2*⊗ *rev1*⊗, ☐ *est2*⊗ *rev7*⊗,☐ *est2*⊗
rad30⊗, ◇ *est2*⊗ *exo1*⊗*,* ☐ *rad30*⊗ *rev7*⊗ and ☐ *est2*⊗ *rad30*⊗ *rev7*⊗ mutant cells at the
indicated time points. Spore colonies of the appropriate genotype were obtained from freshly dissected tetrads of ABX1269, ABX1727 and ABX1729 (Table 1) and dispersed in water. Aliquots were removed to determine viability following dilution, plating on to YPD medium and incubation for three days at 30°. The remainder was plated on to synthetic medium lacking arginine and containing 60 µg/ml canavanine, and incubated for 3 days at 30°. The colonies arising on the canavanine plates were counted, replicaplated
to synthetic medium lacking uracil and the numbers of Ura^- and Ura^+ colonies determined after overnight incubation at 30°. *CAN1* mutation frequency was determined by dividing the number of Can^r Ura^+ colonies by the number of viable cells plated for each spore colony. *CAN1* mutation rate was determined using the median *CAN1* mutation frequency from at least 10 independent trials (Lea and Coulson 1949). Statistical significance was tested by determining the number of trials with each strain that were above and below the group median frequency, and then performing χ^2 analysis
and Fisher's exact test. This process was repeated at five successive growth intervals approximately 25 generations apart using single colonies that arose on the YPD viability plates.

Figure 2. *CYH2* mutation rate does not increase in telomerase deficient cells during replicative senescence. *CYH2* mutation rate of ◆ wild type and ◇ *est2*⊗ mutants was determined at the indicated time points. Wild type and *est2* mutant spore colonies were obtained from freshly dissected tetrads of ABX1429 (Table 1) and dispersed in water. Aliquots were removed to determine viability following dilution, plating on to YPD medium and incubation for three days at 30°. The remainder was plated on to synthetic medium containing 1 µg/ml cycloheximide and incubated for 3 days at 30°. *CYH2* mutation frequency was determined by dividing the number of Cyh_r colonies by the number of viable cells plated for each spore colony. *CYH2* mutation rate was determined
using the median *CYH2* mutation frequency from at least 10 independent trials (Lea and Coulson 1949). Statistical significance was tested by determining the number of trials with each strain that were above and below the group median frequency, and then performing χ^2 analysis and Fisher's exact test. This process was repeated at two additional growth intervals approximately 25 generations apart using single colonies that arose on the YPD viability plates.

Figure 3. Rev1, Rev7 and Rad30 do not significantly affect senescence and subsequent

recovery. **a.** ☐ wild type, ☐ *rev7*⊗, ☐ *rev1*⊗, ☐ *rad30*⊗, **b.** ☐ *est2*⊗, ☐ *est2*⊗ *rev7*⊗, ☐*est2*⊗ *rev1*⊗, ☐*est2*⊗ *rad30*⊗, ☐ *rad30*⊗ *rev7*⊗, and ☐ *est2*⊗ *rad30*⊗ *rev7*⊗**.** Serial liquid growth was performed as described previously (Hackett *et al*. 2001). During each day of serial liquid growth, hemocytometer counts were performed to determine the number of cell bodies, after which approximately 500 cells were plated to YPD and incubated at 30°C for 3 days. Colonies were then counted and divided by 500 to determine plating efficiency. Finally, viability was determined following each day of growth in liquid culture by taking the number of cell bodies, and multiplying by the plating efficiency. Results are the mean ±2SE from at least eight independent samples of each indicated genotype.

Figure1

a

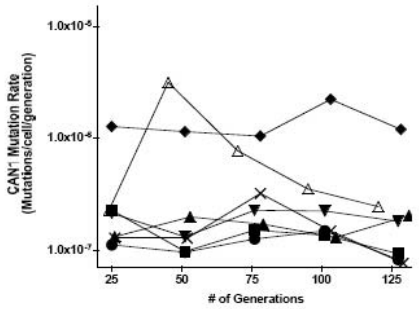
1.0x10⁻⁵
1.0x10⁻⁶
1.0x10⁻⁷
CAN¹ Mutation Rate
(Mutations/cell/generation)
25
50
75
100
125
# of Generations

b

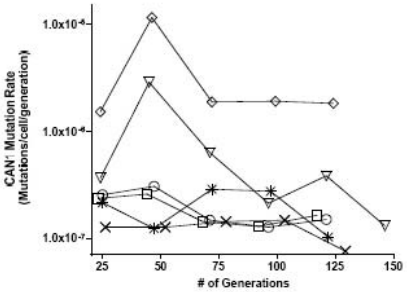
1.0x10⁻⁴
1.0x10⁻⁵
1.0x10⁻⁶
CAN¹ Mutation Rate
(Mutations/cell/generation)
25
50
75
100
125
150
# of Generations

Figure 2

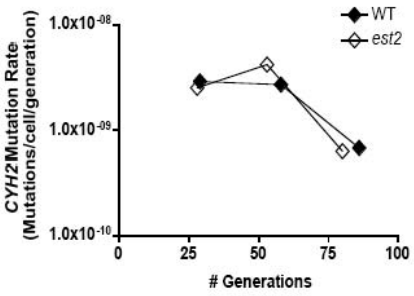
WT
est2
CYH2 Mutation Rate
(Mutations/cell/generation)
1.0x10-08
1.0x10-09
1.0x10-10
0
25
50
75
100
Generations

39

Figure 3

a

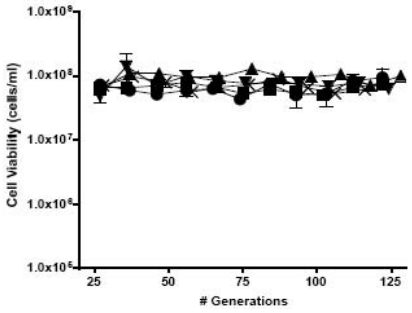

b

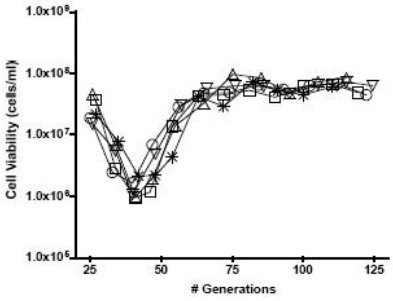

Figure 1 Serial Liquid Growth

Figure 1: *est2 est2 msh2* and WT growth in liquid culture

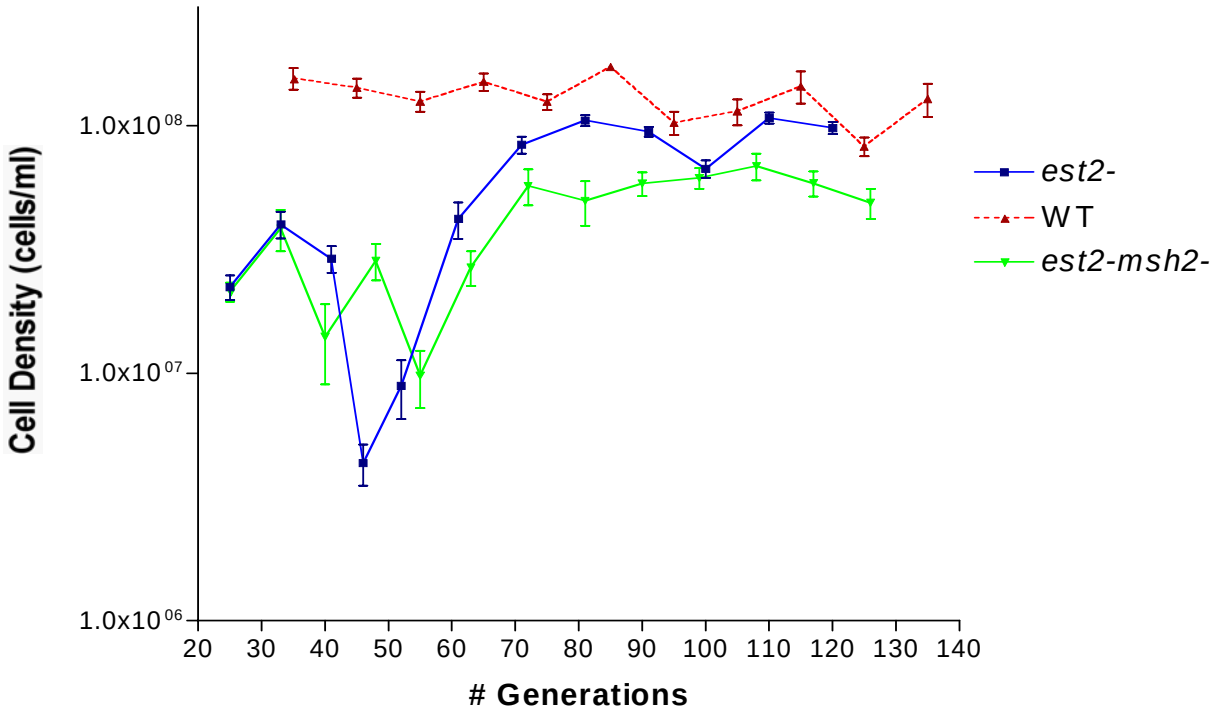

Figure 2 Cell Viability

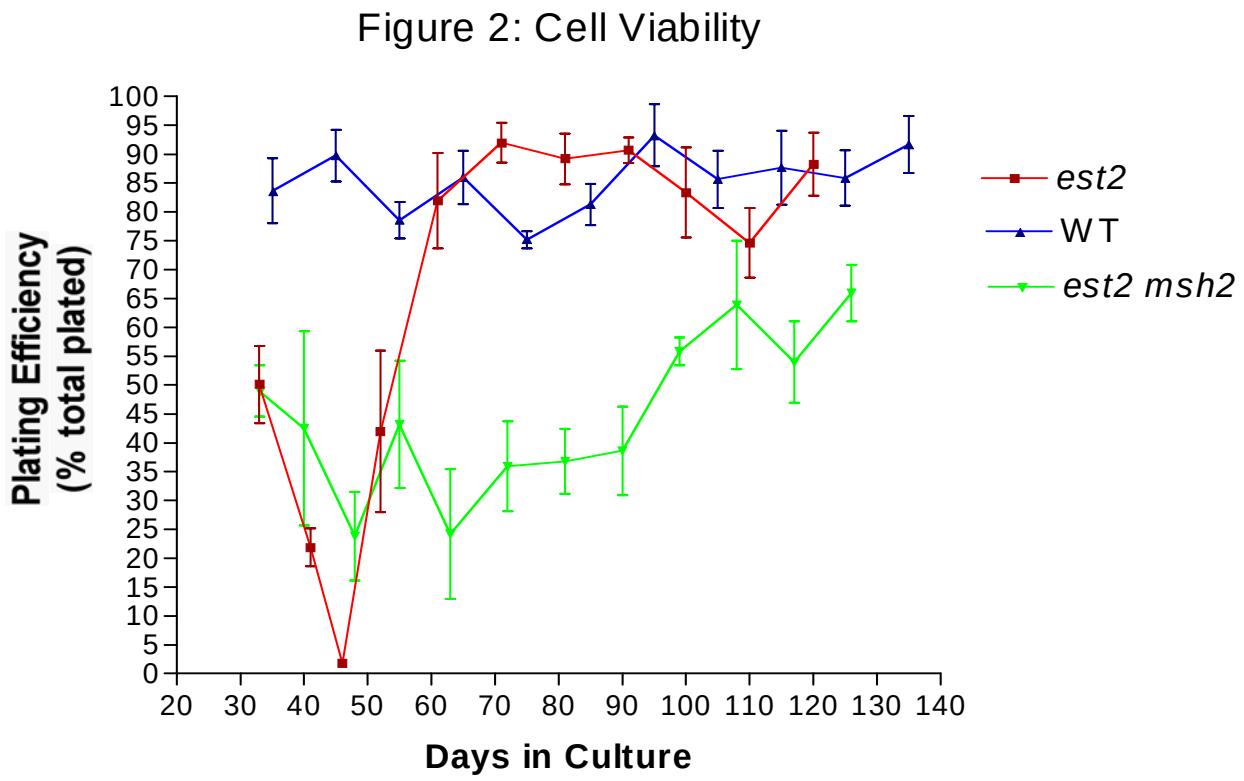

Figure 3 IHE/CL Assay

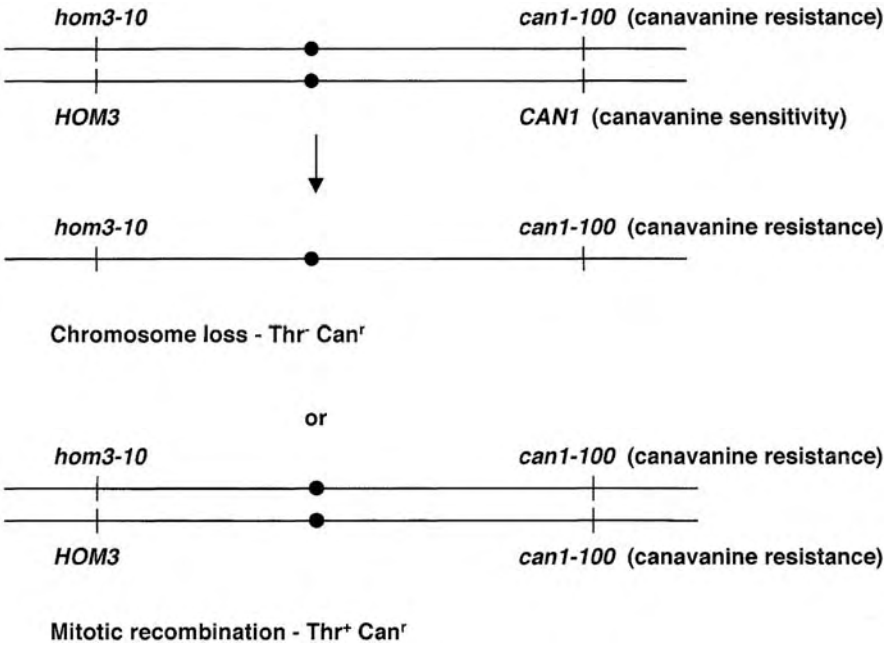

Table 1

Interhomolog Recombination and Chromosome Loss Rates From Cells in Serial Liquid Culture[a]

	25		60		100	
Genotype	IHR[b]	CL[c]	IHR	CL	IHR	CL
WT	4.8×10^{-5} (3.7-5.8)[d] (1)[e]	3.0×10^{-5} (1.7-3.6) (1)	9.2×10^{-5} (8.9-10) (1)	1.6×10^{-5} (1.0-2.2) (1)	2.6×10^{-4} (1.1-3.0) (1)	4.2×10^{-5} (1.7-4.7) (1)
rad30	1.4×10^{-4} (1.2-1.6) (3)	4.7×10^{-5} (2.1-6.0) (1.6)	1.9×10^{-4} (0.8-2.5) (2)	2.1×10^{-5} (0.9-4.4) (1.3)	3.6×10^{-4} (1.5-4.0) (1.4)	5.9×10^{-5} (1.5-9.0) (1.4)
rev7	1.8×10^{-4} (1.2-2.0) (3.7)	4.4×10^{-5} (3.6-5.4) (1.5)	3.7×10^{-4} (3.5-4.0) (3.5)	2.5×10^{-5} (1.8-4.0) (2.8)	$6.\times10^{-4}$ (4.8-7.4) (2.3)	5.8×10^{-5} (3.0-9.3) (1.4)
rad52	8.1×10^{-5} (2.9-16) (1.7)	6.0×10^{-4} (3.0-11) (20)	5.0×10^{-5} (2.8-9.4) (0.5)	7.2×10^{-4} (4.6-7.8) (45)	2.7×10^{-5} (1.6-8.1) (0.1)	9×10^{-4} (4.2-10) (21)
est2	8.3×10^{-5} (3.5-21) (1.1)	3.0×10^{-5} (1.7-6.4) (1)	1.5×10^{-3} (0.9-3.7) (16.3)	1.1×10^{-4} (0.7-3.8) (6.9)	4.0×10^{-4} (2.3-15) (1.5)	2.6×10^{-5} (1.8-4.5) (0.6)
est2 rev7	6.5×10^{-5} (3.8-25) (1.3)	2.4×10^{-5} (1.0-3.0) (1)	7.6×10^{-4} (4.8-9.8) (8.2)	6.0×10^{-5} (1.9-7.5) (3.8)	2.8×10^{-4} (2.2-4.4) (1)	3.7×10^{-5} (2.9-4.8) (1)
est2 rad30	8.2×10^{-5} (4.5-23) (1.7)	1.8×10^{-5} (1.0-3.7) (0.6)	9.1×10^{-4} (6.5-11) (10)	3.1×10^{-5} (2.4-5.8) (2.0)	4.5×10^{-4} (2.4-10) (1.7)	4.0×10^{-5} (2.0-4.4)(1)
~~*est2 rad52*~~	~~3.6×10^{-6} (0.07)~~	~~5.3×10^{-5} (1.8)~~	~~3.0×10^{-6} (0.03)~~	~~7.7×10^{-5}(5)~~	~~NA[f]~~	~~NA~~

[a] Wildtype and homozygous mutant diploids transformed with a wild-type *EST2* gene on a *URA3* selectable plasmid were grown to single colonies on YPD medium then replica plated to *ura-* medium to select for colonies that had evicted the plasmid. Freshly isolated *ura-,* YPD colonies were dispersed in water, cell number assessed by hemacytometer counts, viability determined by plating on to YPD, and interhomolog recombination and chromosome loss determined by plating to synthetic complete medium containing canavanine. Serial liquid cultures were started by inoculating 5 ml YPD cultures with 5×10^5 cells that were grown for 20hr and processed as above. The 25 generation timepoint is before senescence. By 60 generations, the *est2* mutant cultures had reached senescence, and recovered by 100 generations.

[b] Appropriate dilutions of the original colonies dispersed in water, and the 20hr YPD cultures were plated on medium containing canavanine. Canavanine resistant colonies were counted and replica plated to medium lacking threonine. The number of canavanine resistant threonine prototrophs was used to determine the rate of interhomolog recombination (IHR) by the method of the median from at least 9 independent cultures.

[c] Chromosome loss rates were determined from the number of colonies that were canavanine resistant threonine auxotrophs (CL) using the method of the median.

[d] Confidence intervals of >95% were determined using a table developed by william knight.

[e] Fold difference from wild-type.

[f] No recovery.

Figure 4

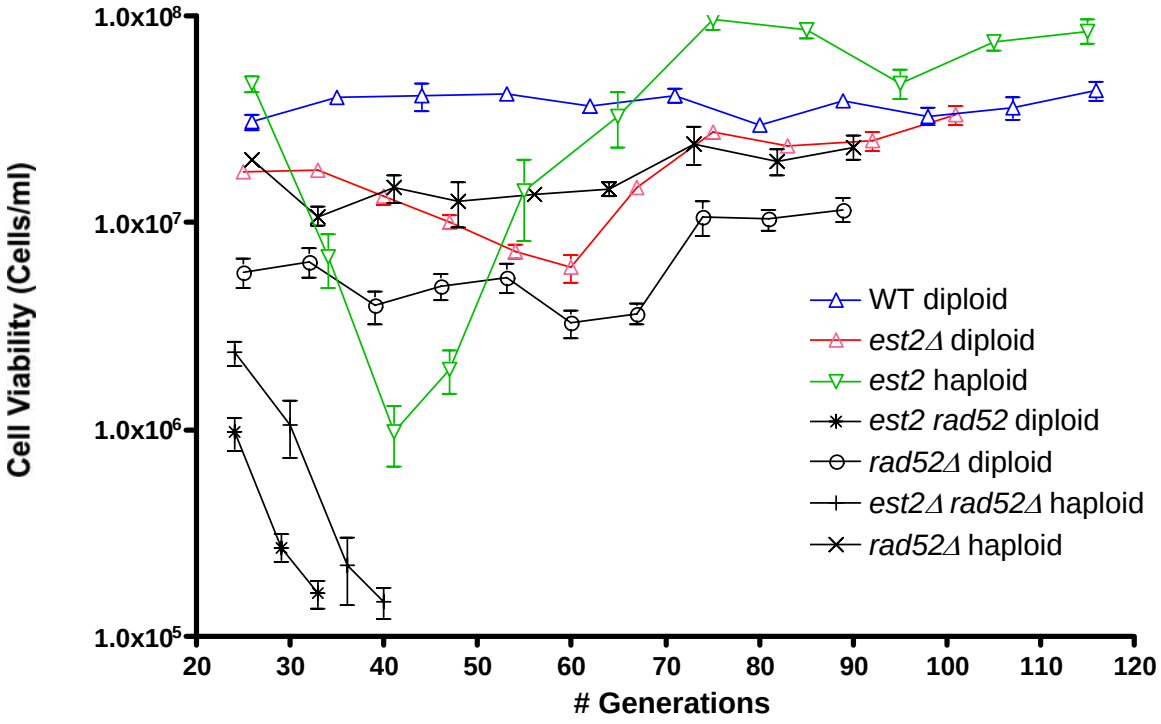
1.0x10^8
1.0x10^7
1.0x10^6
1.0x10^5
Cell Viability (Cells/ml)
20
30
40
50
60
70
80
90
100
110
120
Generations
WT diploid
est2Δ diploid
est2 haploid
est2 rad52 diploid
rad52Δ diploid
est2Δ rad52Δ haploid
rad52Δ haploid

Figure 5

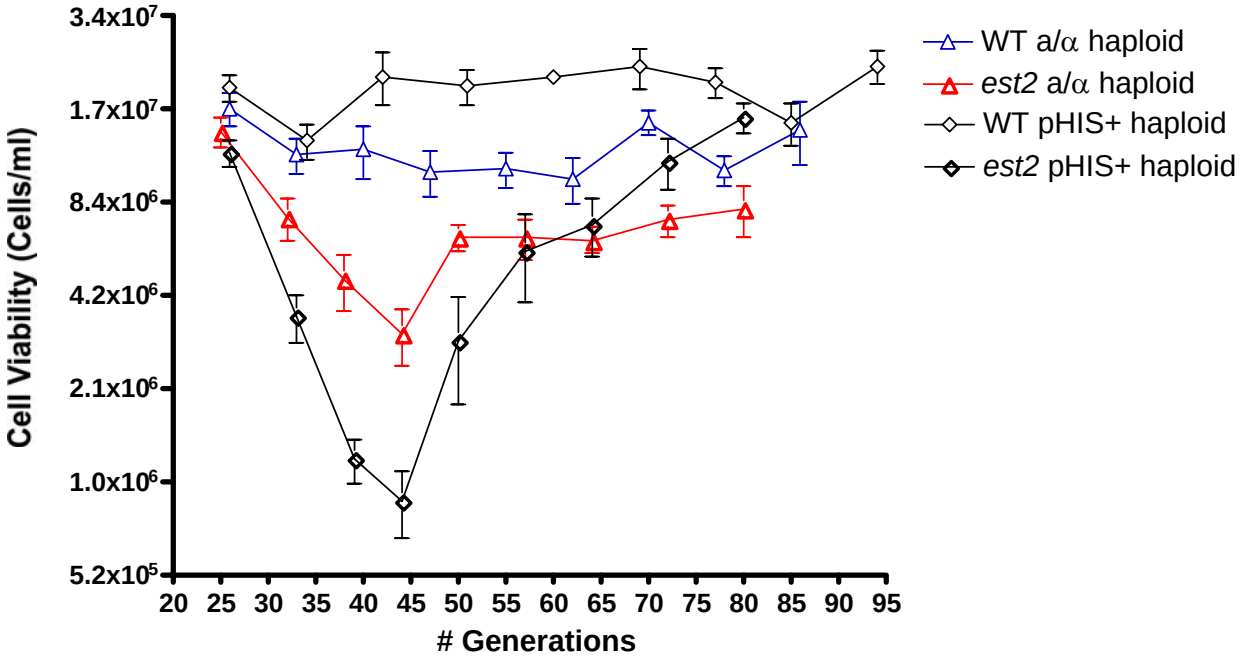
Cell Viability (Cells/ml)
3.4x10^7
1.7x10^7
8.4x10^6
4.2x10^6
2.1x10^6
1.0x10^6
5.2x10^5
20 25 30 35 40 45 50 55 60 65 70 75 80 85 90 95
Generations
WT a/α haploid
est2 a/α haploid
WT pHIS+ haploid
est2 pHIS+ haploid

Figure 6

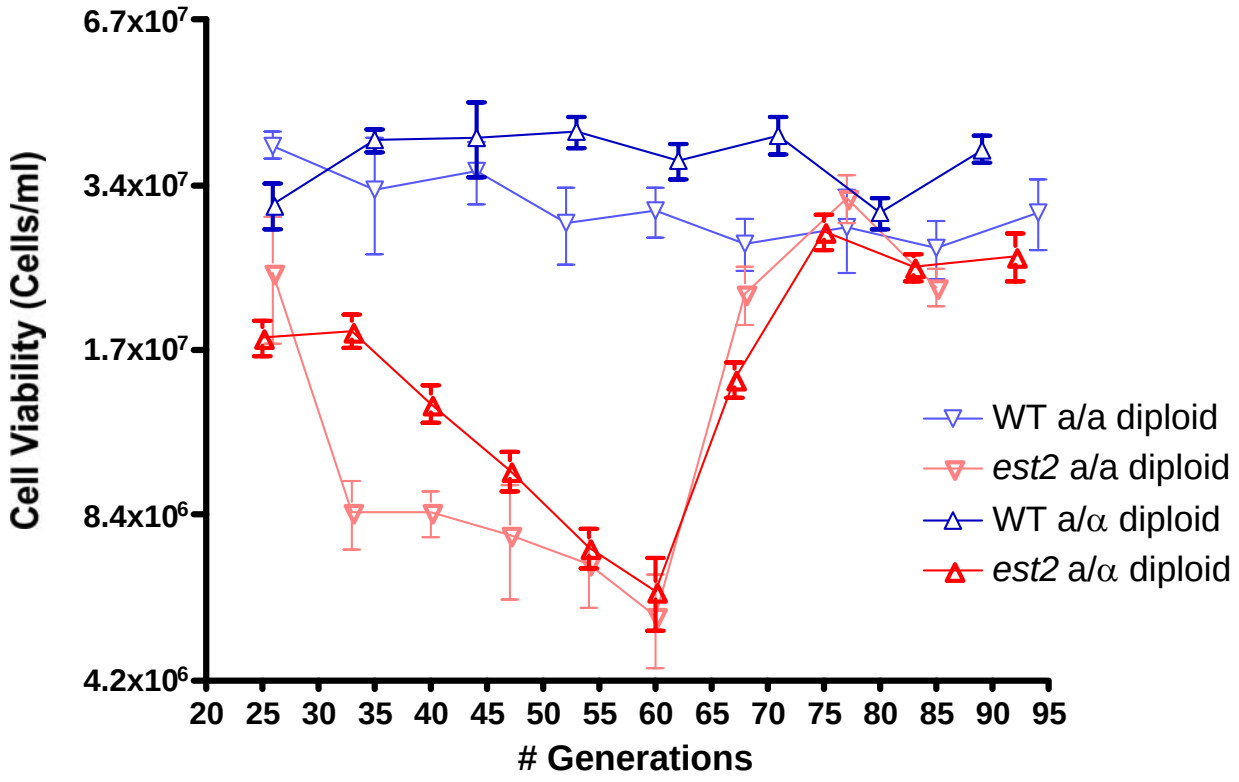
6.7x10^7
3.4x10^7
1.7x10^7
8.4x10^6
4.2x10^6
Cell Viability (Cells/ml)
20 25 30 35 40 45 50 55 60 65 70 75 80 85 90 95
Generations
WT a/a diploid
est2 a/a diploid
WT a/α diploid
est2 a/α diploid

Figure 7

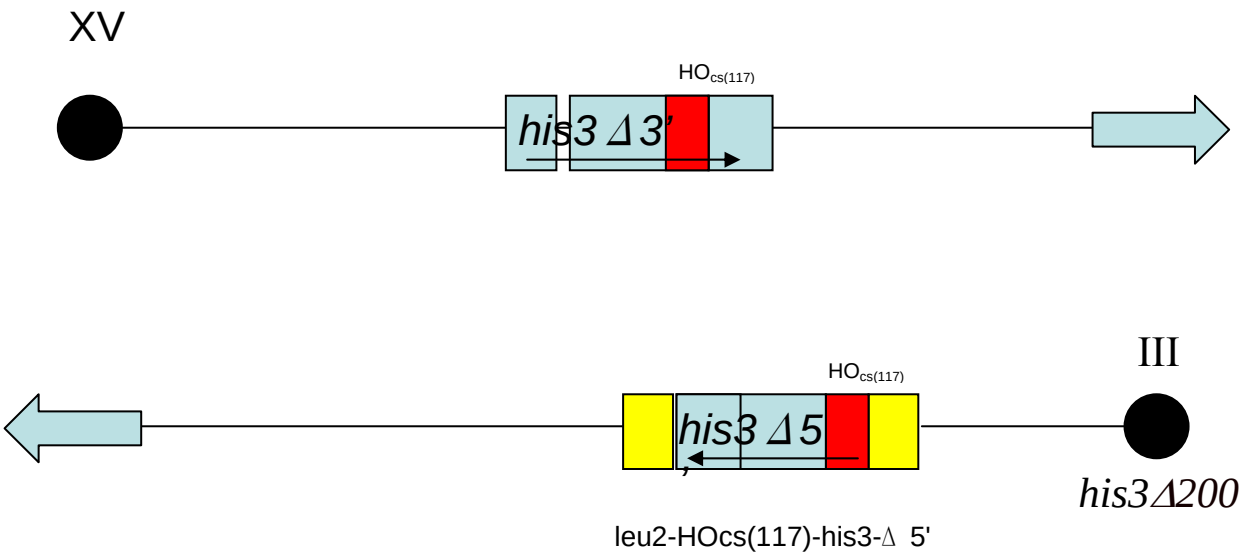

leu2-HOcs(117)-his3-Δ 5'

Figure 8

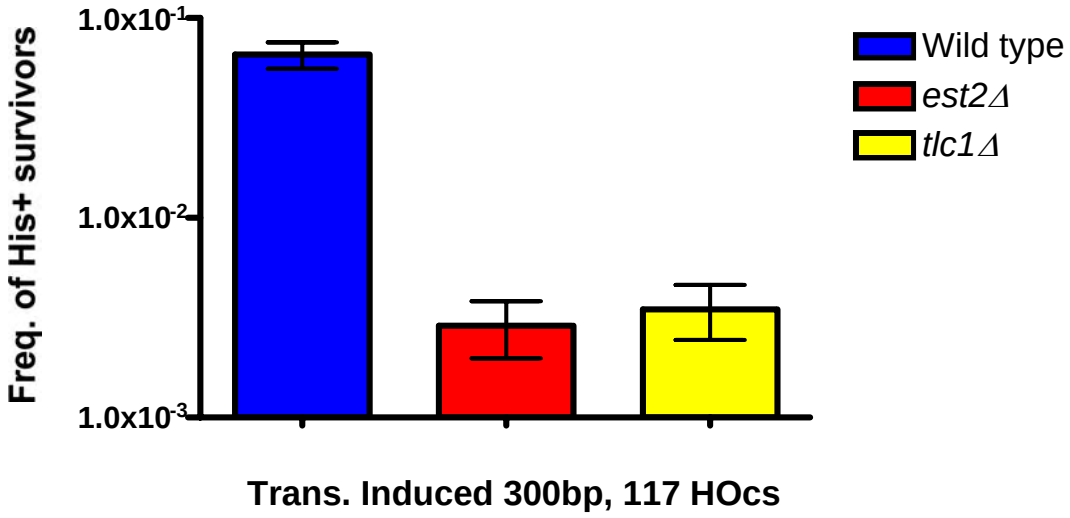

- **25 Generations**

Figure 9

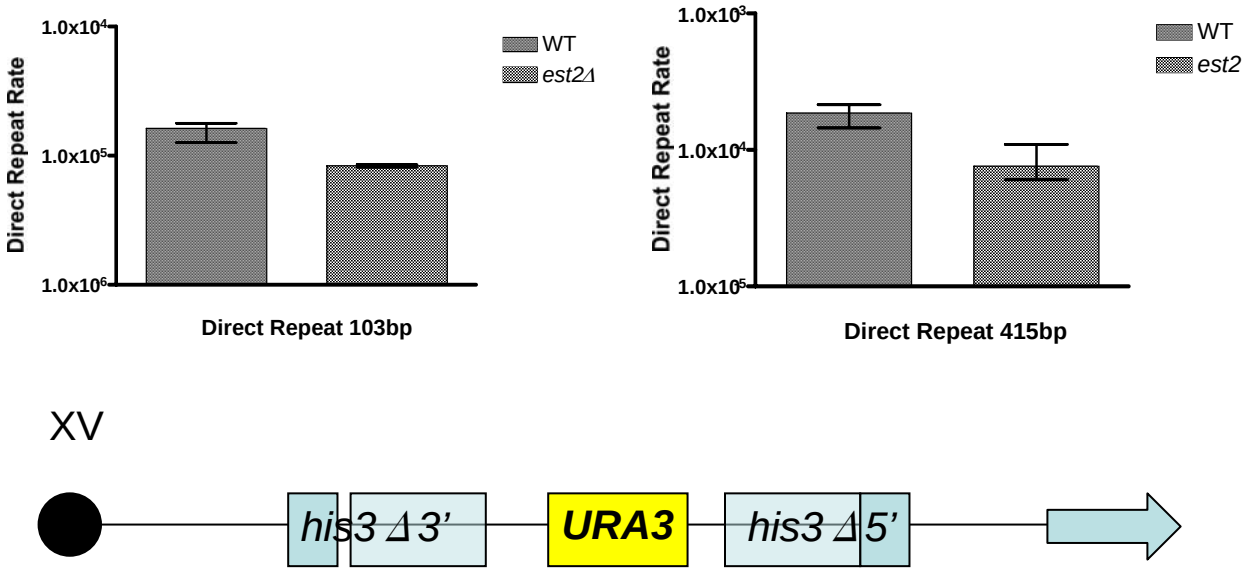
1.0x10^4
1.0x10^5
1.0x10^6
Direct Repeat Rate
WT
est2Δ
Direct Repeat 103bp
1.0x10^3
1.0x10^4
1.0x10^5
Direct Repeat Rate
WT
est2
Direct Repeat 415bp
XV
his3 Δ 3'
URA3
his3 Δ 5'